

The strong vertices of charmed mesons D, D^* and charmonia $J/\psi, \eta_c$

Jie Lu¹, Guo-Liang Yu^{1,*} and Zhi-Gang Wang^{1†}

Department of Mathematics and Physics, North China Electric power university, Baoding 071003, People's Republic of China

(Dated: May 9, 2023)

In this work, the strong form factors and coupling constants of the vertices $DDJ/\psi, DD^*J/\psi, D^*D^*J/\psi, DD^*\eta_c, D^*D^*\eta_c$ are calculated within the framework of the QCD sum rule. For each vertex, we analyze the form factor considering all possible off-shell cases and the contributions of the vacuum condensate terms $\langle\bar{q}q\rangle, \langle\bar{q}g_s\sigma Gq\rangle, \langle g_s^2 G^2\rangle, \langle f^3 G^3\rangle$ and $\langle\bar{q}\bar{q}\rangle\langle g_s^2 G^2\rangle$. Then, the form factors are fitted into analytical functions $g(Q^2)$ and are extrapolated into time-like regions to get the strong coupling constants. Finally, the strong coupling constants are obtained by using on-shell cases of the intermediate mesons ($Q^2 = -m^2$). The results are as follows, $g_{DDJ/\psi} = 5.01^{+0.58}_{-0.16}$, $g_{DD^*J/\psi} = 3.55^{+0.20}_{-0.21} \text{ GeV}^{-1}$, $g_{D^*D^*J/\psi} = 5.10^{+0.59}_{-0.43}$, $g_{DD^*\eta_c} = 3.68^{+0.39}_{-0.11}$ and $g_{D^*D^*\eta_c} = 4.87^{+0.42}_{-0.40} \text{ GeV}^{-1}$.

I. INTRODUCTION

In recent years, many exotic particles which are beyond the usual quark-model were observed in experiments[1–13]. Some of them have exotic quantum numbers and were interpreted as tetraquark states, pentaquark states, hadron molecular states, quark-gluon hybrids, glueballs and many others[14–22]. The composition of these exotic particles can not be determined only by the mass spectrum. We need to further study their production processes or decay behaviours, where the form factor and coupling constant become particularly important. For example, the exotic states $D_{s0}^*(2317)$ and $D_{s1}(2460)$ were discovered in the decay processes $B \rightarrow \bar{D}^{(*)}D_{s0}^*(2317)$ and $B \rightarrow \bar{D}^{(*)}D_{s1}(2460)$ [1, 23, 24], and their decay branching fractions were also measured in the experiment[25]. If they are interpreted as $D^{(*)}K$ or $D_s^{(*)}\eta$ molecular states, their production processes can be studied in the triangle mechanism[26], which are shown in Figs. 1 and 2. Under this mechanism, the three meson vertices $DD^*\eta, D^*D^*\eta, DDJ/\psi, D^*D^*J/\psi, DD^*\eta_c$ and $D^*D^*\eta_c$ are especially important for us to analyze their production processes.

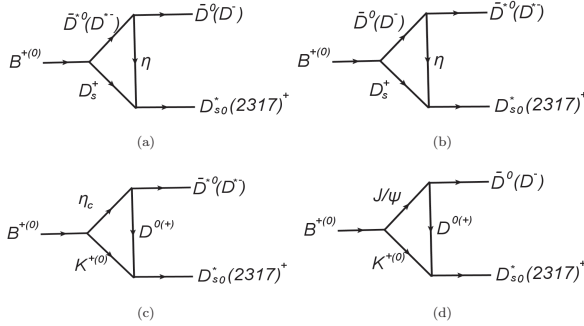


FIG. 1: Triangle diagrams accounting for the B decays: (a) $B^{+(0)} \rightarrow D_s^+\bar{D}^{*0}(D^{*-}) \rightarrow D_{s0}^*(2317)^+\bar{D}^0(D^-)$, (b) $B^{+(0)} \rightarrow D_s^+\bar{D}^0(D^-) \rightarrow D_{s0}^*(2317)^+\bar{D}^{*0}(D^{*-})$, (c) $B^{+(0)} \rightarrow \eta_c K^{+(0)} \rightarrow D_{s0}^*(2317)^+\bar{D}^{*0}(D^{*-})$ and (d) $B^{+(0)} \rightarrow J/\psi K^{+(0)} \rightarrow D_{s0}^*(2317)^+\bar{D}^0(D^-)$.

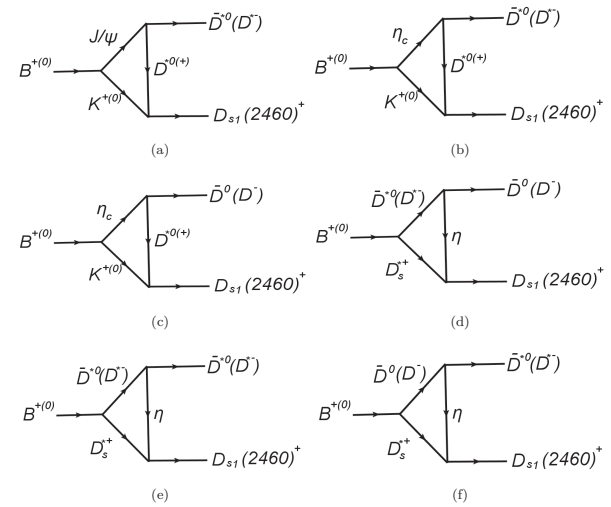


FIG. 2: Triangle diagrams accounting for the B decays: (a) $B^{+(0)} \rightarrow J/\psi K^{+(0)} \rightarrow D_{s1}(2460)^+\bar{D}^{*0}(D^{*-})$, (b) $B^{+(0)} \rightarrow \eta_c K^{+(0)} \rightarrow D_{s1}(2460)^+\bar{D}^{*0}(D^{*-})$, (c) $B^{+(0)} \rightarrow \eta_c K^{+(0)} \rightarrow D_{s1}(2460)\bar{D}^0(D^-)$, (d) $B^{+(0)} \rightarrow D_s^+\bar{D}^-(D^{*-}) \rightarrow D_{s1}(2460)^+\bar{D}^0(D^-)$, (e) $B^{+(0)} \rightarrow D_s^+\bar{D}^-(D^{*-}) \rightarrow D_{s1}(2460)^+\bar{D}^{*0}(D^{*-})$ and (f) $B^{+(0)} \rightarrow D_s^+\bar{D}^0(D^-) \rightarrow D_{s1}(2460)^+\bar{D}^{*0}(D^{*-})$.

The QCD is perturbative field theory which has been successfully applied in the high energy region. However, the strong coupling constant between the hadrons lies in the low energy region, which can not be studied by perturbative method. As for the mesons composed of u, d or s quark, the couplings between these mesons have been constrained by the SU(3) chiral symmetry and phenomenological analyses of low energy reactions[27–29]. For the charmed mesons, we can use SU(4) chiral symmetry and phenomenological analysis to get the interaction Lagrangian[30–32]. Because the mass of c quark is much heavier than u, d and s quark, the SU(4) chiral symmetry is badly broken. Therefore, the accurately calculation of the strong coupling constants is of great significance to the study of the destruction of SU(4) chiral symmetry.

Since the strong interaction is non-perturbative in the low energy region, it is difficult to calculate the strong form factors and coupling constants from the QCD first principle. Except for lattice caculation[33, 34], some phenomenological methods are usually employed to carry out this work such

*Electronic address: yuguoliang2011@163.com

†Electronic address: zgwang@aliyun.com

as the QCDSR[35–44], LCSR[45–50], VMD model[31, 32] and other methods[51, 52]. The QCDSR[53] is one of the most powerful non-perturbative methods to analyze the strong vertices. In our previous work, we have analyzed the vertices $D_s^*D_s\phi$, $D_2^*D^*\pi$, $D_{s2}^*D^*K$, $D_2^*D\rho$, $D_2^*D\omega$, $D_{s2}^*D_s\phi$ using the three-point correlation[42, 54, 55]. As a continuation of these tasks, we systematically analyze the strong vertices of the charmed mesons D , D^* and the charmonia J/ψ , η_c using the three-point QCDSR. Although some strong vertices DDJ/ψ , DD^*J/ψ , D^*D^*J/ψ and $DD^*\eta_c$ were already analyzed by other collaborations in QCDSR[56, 57]. However, the high dimension condensate terms such as the $\langle\bar{q}g_s\sigma Gq\rangle$, $\langle f^3G^3 \rangle$ and $\langle\bar{q}q\rangle\langle g_s^2G^2 \rangle$ were neglected in their studies, which is significant to the accuracy of the final results.

This article is organized as follows. After the introduction in Sec. I, we analyze the strong vertices DDJ/ψ , DD^*J/ψ , D^*D^*J/ψ , $DD^*\eta_c$ and $D^*D^*\eta_c$ with the QCDSR in Sec. II. In these analyses, all off-shell cases of the intermediate mesons are considered. In the QCD side, we consider the perturbative contribution and vacuum condensate terms $\langle\bar{q}q\rangle$, $\langle\bar{q}g_s\sigma Gq\rangle$, $\langle g_s^2G^2 \rangle$, $\langle f^3G^3 \rangle$ and $\langle\bar{q}q\rangle\langle g_s^2G^2 \rangle$. In Sec. III, we present the numerical results and discussions. Sec. IV is reserved for our conclusions. Some important figures and formulas will be shown in the Appendixes A-C.

II. QCD SUM RULES

Firstly, we write down the three-point correlation function,

$$\begin{aligned} \Pi(p, p') = & i^2 \int d^4x d^4y e^{ip'x} e^{i(p-p')y} \\ & \times \langle 0 | T\{J_C(x)J_B(y)J_A^\dagger(0)\} | 0 \rangle \end{aligned} \quad (1)$$

where T denotes the time ordered product and J_A^\dagger , J_B and J_C are the meson interpolating currents. The subscripts A, B, and C denote three mesons in each vertex, where B is the intermediate meson and is off-shell. Assignments of the mesons for each vertex are presented in Table I.

TABLE I: The assignments of the mesons A, B and C for each vertex where B denotes the off-shell mesons.

Vertices	A	B(off-shell)	C
DDJ/ψ	D	J/ψ	D
	D	D	J/ψ
DD^*J/ψ	D^*	J/ψ	D
	D^*	D	J/ψ
	D	D^*	J/ψ
D^*D^*J/ψ	D^*	J/ψ	D^*
	D^*	D^*	J/ψ
$DD^*\eta_c$	D	η_c	D^*
	D^*	D	η_c
	D	D^*	η_c
$D^*D^*\eta_c$	D^*	η_c	D^*
	D^*	D^*	η_c

The meson interpolating currents in these analyses are as

follows,

$$\begin{aligned} J_D(x) &= \bar{u}(x)i\gamma_5 c(x) \\ J_{D^*}(x) &= \bar{u}(x)\gamma_\mu c(x) \\ J_{J/\psi}(x) &= \bar{c}(x)\gamma_\mu c(x) \\ J_{\eta_c}(x) &= \bar{c}(x)i\gamma_5 c(x) \end{aligned} \quad (2)$$

In the framework of QCD sum rule, the correlation function is firstly calculated in two levels: the hadron level which is called the phenomenological side, and the quark level which is called the QCD side. Then we use the quark hadron duality coordinate the calculation of these two levels. In the following section, we will obtain the sum rules about these strong vertices.

A. The Phenomenological side

In phenomenological side, we insert complete sets of hadronic states with the same quantum numbers as the current J_A^\dagger , J_B and J_C into the correlation function,

$$\begin{aligned} \Pi(p, p') = & \frac{\langle 0 | J_C(0) | C(p') \rangle \langle 0 | J_B(0) | B(q) \rangle}{(m_A^2 - p^2)(m_C^2 - p'^2)(m_B^2 - q^2)} \\ & \times \langle A(p) | J_A^\dagger(0) | 0 \rangle \langle B(q) C(p') | A(p) \rangle + h.c \end{aligned} \quad (3)$$

where $h.c$ represents the contributions of higher resonances and continuum states of each meson. A, B, and C stand for mesons in each vertex which are already shown in Table I. The meson vacuum matrix elements appearing in this equation are substituted by the following parameterized equations,

$$\begin{aligned} \langle 0 | J_D(0) | D \rangle &= \frac{f_D m_D^2}{m_c} \\ \langle 0 | J_{D^*}(0) | D^* \rangle &= f_{D^*} m_{D^*} \epsilon_\mu \\ \langle 0 | J_{J/\psi}(0) | J/\psi \rangle &= f_{J/\psi} m_{J/\psi} \xi_\mu \\ \langle 0 | J_{\eta_c}(0) | \eta_c \rangle &= \frac{f_{\eta_c} m_{\eta_c}^2}{2m_c^2} \end{aligned} \quad (4)$$

where f_D , f_{D^*} , $f_{J/\psi}$ and f_{η_c} are the meson decay constants, ϵ_μ and ξ_μ are the polarization vectors of D^* and J/ψ , respectively. All of the meson vertex matrix elements in our calculations can be obtained by using the effective Lagrangian in Eq. (5) [58, 59],

$$\begin{aligned} \mathcal{L}_{DDJ/\psi} &= ig_{DDJ/\psi} \psi_\mu (\partial^\mu D \bar{D} - D \partial^\mu \bar{D}) \\ \mathcal{L}_{DD^*J/\psi} &= -g_{D^*DJ/\psi} \epsilon^{\alpha\beta\sigma\rho} \partial_\alpha \psi_\beta (\partial_\sigma D_\rho^* \bar{D} + D \partial_\sigma \bar{D}_\rho^*) \\ \mathcal{L}_{D^*D^*J/\psi} &= ig_{D^*D^*J/\psi} [\psi^\alpha (\partial_\alpha D^{*\beta} \bar{D}_\beta^* - D^{*\beta} \partial_\alpha \bar{D}_\beta^*) \\ &+ (\partial_\alpha \psi_\beta D^{*\beta} - \psi_\beta \partial_\alpha D^{*\beta}) \bar{D}^{*\alpha} + D^{*\alpha} (\psi^\beta \partial_\alpha \bar{D}_\beta^* - \partial_\alpha \psi_\beta \bar{D}^{*\beta})] \\ \mathcal{L}_{DD^*\eta_c} &= ig_{D^*D^*\eta_c} [D^{*\alpha} (\partial_\alpha \eta_c \bar{D} - \eta_c \partial_\alpha \bar{D}) \\ &+ (\partial_\alpha \eta_c D - \eta_c \partial_\alpha D) \bar{D}^{*\alpha}] \\ \mathcal{L}_{D^*D^*\eta_c} &= -g_{D^*D^*\eta_c} \epsilon^{\alpha\beta\sigma\rho} \partial_\alpha D_\beta^* \partial_\sigma \bar{D}_\rho^* \eta_c \end{aligned} \quad (5)$$

Full expressions of the meson vertex elements for all vertices and off-shell cases are as follows,

$$\begin{aligned}
\langle D(p')J/\psi(q)|D(p)\rangle &= g_{DDJ/\psi}^{J/\psi}(q^2)\xi_\nu^*(p+p')^\nu \\
\langle D(q)J/\psi(p')|D(p)\rangle &= g_{DDJ/\psi}^D(q^2)\xi_\mu(p+q)^\mu \\
\langle D(p')J/\psi(q)|D^*(p)\rangle &= -g_{DD^*J/\psi}^{J/\psi}(q^2)\epsilon^{\sigma\alpha\beta\rho}p_\sigma p'_\alpha\xi_\beta\xi_\rho \\
\langle D(q)J/\psi(p')|D^*(p)\rangle &= -g_{DD^*J/\psi}^D(q^2)\epsilon^{\sigma\alpha\beta\rho}p_\sigma p'_\alpha\xi_\beta\xi_\rho \\
\langle D^*(q)J/\psi(p')|D(p)\rangle &= -g_{DD^*J/\psi}^{D^*}(q^2)\epsilon^{\alpha\beta\sigma\rho}p_a q_\sigma \xi_\beta \xi_\rho \\
\langle D^*(p')J/\psi(q)|D^*(p)\rangle &= g_{D^*D^*J/\psi}^{J/\psi}[(p_\alpha + p'_\alpha)\zeta^\beta \epsilon_\beta^* \xi^{*\alpha} \\
&\quad -(p_\alpha + q_\alpha)\xi_\beta^* \zeta^\beta \epsilon^{*\alpha} - (p'_\alpha - q_\alpha)\zeta^\alpha \xi^{*\beta} \epsilon_\beta^*] \\
\langle D^*(q)J/\psi(p')|D^*(p)\rangle &= g_{D^*D^*J/\psi}^{D^*}[(p_\alpha + q_\alpha)\zeta^\beta \epsilon_\beta^* \xi^{*\alpha} \\
&\quad -(p_\alpha + p'_\alpha)\xi_\beta^* \zeta^\beta \epsilon^{*\alpha} - (q_\alpha - p'_\alpha)\zeta^\alpha \xi^{*\beta} \epsilon_\beta^*] \\
\langle D(p')\eta_c(q)|D^*(p)\rangle &= -g_{DD^*\eta_c}^{\eta_c}(q^2)\zeta^\alpha(q_\alpha - p'_\alpha) \\
\langle D(q)\eta_c(p')|D^*(p)\rangle &= -g_{DD^*\eta_c}^D(q^2)\zeta^\alpha(p'_\alpha - q_\alpha) \\
\langle D^*(q)\eta_c(p')|D(p)\rangle &= -g_{DD^*\eta_c}^{D^*}(q^2)(p_\alpha + p'_\alpha)\xi^{*\alpha} \\
\langle D^*(p')\eta_c(q)|D^*(p)\rangle &= -g_{D^*D^*\eta_c}^{\eta_c}(q^2)\epsilon^{\alpha\beta\sigma\rho}p_\alpha p'_\sigma \zeta_\beta \epsilon_\rho^* \\
\langle D^*(q)\eta_c(p')|D^*(p)\rangle &= -g_{D^*D^*\eta_c}^{D^*}(q^2)\epsilon^{\alpha\beta\sigma\rho}p_\alpha q_\sigma \epsilon_\beta \zeta_\rho^* \quad (6)
\end{aligned}$$

where ξ_μ, ζ_μ and ϵ_μ are the meson polarization vectors, and $q = p - p'$. The superscript of g in these equations denotes the off-shell meson, and subscript denotes the vertex. For example, $g_{DDJ/\psi}^{J/\psi}$ represents the strong coupling constant of the vertex DDJ/ψ , where J/ψ is the intermediate meson and is off-shell. From Eqs. (4)-(6), the correlation functions in hadron side will be obtained, and it can be expanded into different tensor structures. Theoretically, different tensor structures for a correlation function will lead to the same result, thus we can choose a certain tensor structure to obtain the sum rules.

B. The QCD side

In QCD side, we do the operator product expansion(OPE) of the correlation function by contracting the quark fields with Wick's theorem. The correlation functions in QCD side for vertices DDJ/ψ , DD^*J/ψ , D^*D^*J/ψ , $DD^*\eta_c$ and $D^*D^*\eta_c$ for all off-shell cases are shown in Eqs. (7)-(11) respectively,

$$\begin{aligned}
\Pi_\mu^{J/\psi}(p, p') &= \int d^4x d^4y e^{ip'x} e^{i(p-p')y} \\
&\quad \times Tr\{C^{nk}(y)\gamma_5 U^{km}(-x)\gamma_5 C^{mn}(x-y)\gamma_\mu\} \\
\Pi_\mu^D(p, p') &= \int d^4x d^4y e^{ip'x} e^{i(p-p')y} \\
&\quad \times Tr\{\gamma_\mu C^{nk}(x)\gamma_5 U^{km}(-y)\gamma_5 C^{mn}(y-x)\} \quad (7)
\end{aligned}$$

$$\begin{aligned}
\Pi_{\mu\nu}^{J/\psi}(p, p') &= -i \int d^4x d^4y e^{ip'x} e^{i(p-p')y} \\
&\quad \times Tr\{C^{nk}(y)\gamma_\nu U^{km}(-x)\gamma_5 C^{mn}(x-y)\gamma_\mu\} \\
\Pi_{\mu\nu}^D(p, p') &= -i \int d^4x d^4y e^{ip'x} e^{i(p-p')y} \\
&\quad \times Tr\{\gamma_\mu C^{nk}(x)\gamma_\nu U^{km}(-y)\gamma_5 C^{mn}(y-x)\} \\
\Pi_{\mu\nu}^{D^*}(p, p') &= -i \int d^4x d^4y e^{ip'x} e^{i(p-p')y} \\
&\quad \times Tr\{\gamma_\mu C^{nk}(x)\gamma_5 U^{km}(-y)\gamma_\nu C^{mn}(y-x)\} \quad (8)
\end{aligned}$$

$$\begin{aligned}
\Pi_{\mu\nu\sigma}^{J/\psi}(p, p') &= \int d^4x d^4y e^{ip'x} e^{i(p-p')y} \\
&\quad \times Tr\{C^{nk}(y)\gamma_\nu U^{km}(-x)\gamma_\sigma C^{mn}(x-y)\gamma_\mu\} \\
\Pi_{\mu\nu\sigma}^{D^*}(p, p') &= \int d^4x d^4y e^{ip'x} e^{i(p-p')y} \\
&\quad \times Tr\{\gamma_\mu C^{nk}(x)\gamma_\sigma U^{km}(-y)\gamma_\nu C^{mn}(y-x)\} \quad (9)
\end{aligned}$$

$$\begin{aligned}
\Pi_\mu^{\eta_c}(p, p') &= \int d^4x d^4y e^{ip'x} e^{i(p-p')y} \\
&\quad \times Tr\{C^{nk}(y)\gamma_\mu U^{km}(-x)\gamma_5 C^{mn}(x-y)\gamma_5\} \\
\Pi_\mu^D(p, p') &= \int d^4x d^4y e^{ip'x} e^{i(p-p')y} \\
&\quad \times Tr\{\gamma_5 C^{nk}(x)\gamma_\mu U^{km}(-y)\gamma_5 C^{mn}(y-x)\} \\
\Pi_\mu^{D^*}(p, p') &= \int d^4x d^4y e^{ip'x} e^{i(p-p')y} \\
&\quad \times Tr\{\gamma_5 C^{nk}(x)\gamma_5 U^{km}(-y)\gamma_\mu C^{mn}(y-x)\} \quad (10)
\end{aligned}$$

$$\begin{aligned}
\Pi_{\mu\nu}^{\eta_c}(p, p') &= -i \int d^4x d^4y e^{ip'x} e^{i(p-p')y} \\
&\quad \times Tr\{C^{nk}(y)\gamma_\nu U^{km}(-x)\gamma_\mu C^{mn}(x-y)\gamma_5\} \\
\Pi_{\mu\nu}^{D^*}(p, p') &= -i \int d^4x d^4y e^{ip'x} e^{i(p-p')y} \\
&\quad \times Tr\{\gamma_5 C^{nk}(x)\gamma_\nu U^{km}(-y)\gamma_\mu C^{mn}(y-x)\} \quad (11)
\end{aligned}$$

It is the same as g in Eqs. (4)-(6), the superscript of Π in these above equations denotes the meson which is off-shell. $U^{ij}(x)$

and $C^{ij}(x)$ are the full propagators of $u(d)$ and c quark[60],

$$\begin{aligned}
U^{ij}(x) &= \frac{i\delta^{ij}\not{k}}{2\pi^2 x^4} - \frac{\delta^{ij}m_q}{4\pi^2 x^4} - \frac{\delta^{ij}\langle\bar{q}q\rangle}{12} + \frac{i\delta^{ij}\not{x}m_q\langle\bar{q}q\rangle}{48} \\
&- \frac{\delta^{ij}x^2\langle\bar{q}g_s\sigma Gq\rangle}{192} + \frac{i\delta^{ij}x^2\not{x}m_q\langle\bar{q}g_s\sigma Gq\rangle}{1152} \\
&- \frac{ig_sG_{\alpha\beta}^n t_{ij}^n(\not{x}\sigma^{\alpha\beta} + \sigma^{\alpha\beta}\not{x})}{32\pi^2 x^2} - \frac{i\delta^{ij}x^2\not{x}g_s^2\langle\bar{q}q\rangle^2}{7776} \\
&- \frac{\delta^{ij}x^4\langle\bar{q}q\rangle\langle g_s^2 GG \rangle}{27648} - \frac{\langle\bar{q}^j\sigma^{\mu\nu}q^i\rangle\sigma_{\mu\nu}}{8} \\
&- \frac{\langle\bar{q}^j\gamma^\mu q^i\rangle\gamma_\mu}{4} + \dots \\
C^{ij}(x) &= \frac{i}{(2\pi)^4} \int d^4k e^{-ik\cdot x} \left\{ \frac{\delta^{ij}}{\not{k}-m_c} \right. \\
&- \frac{g_s G_{\alpha\beta}^n t_{ij}^n \sigma^{\alpha\beta}(\not{k}+m_c) + (\not{k}+m_c)\sigma^{\alpha\beta}}{4(k^2-m_c^2)^2} \\
&+ \frac{g_s D_\alpha G_{\beta\lambda}^n t_{ij}^n (f^{\lambda\beta\alpha} + f^{\lambda\alpha\beta})}{3(k^2-m_c^2)^4} \\
&- \frac{g_s^2 (t^a t^b)_{ij} G_{\alpha\beta}^a G_{\mu\nu}^b (f^{\alpha\beta\mu\nu} + f^{\alpha\mu\beta\nu} + f^{\alpha\mu\nu\beta})}{4(k^2-m_c^2)^5} \\
&\left. + \dots \right\} \quad (12)
\end{aligned}$$

where $\langle g_s^2 G^2 \rangle = \langle g_s^2 G_{\alpha\beta}^n G^{n\alpha\beta} \rangle$, $D_\alpha = \partial_\alpha - ig_s G_{\alpha\beta}^n t^n$, $t^n = \frac{\lambda^n}{2}$, λ^n is the Gell-Mann matrix, i, j are color indices, $q = u(d)$, $\sigma_{\alpha\beta} = \frac{i}{2}[\gamma_\alpha, \gamma_\beta]$ and $f^{\lambda\alpha\beta}$, $f^{\alpha\beta\mu\nu}$ have the following forms,

$$f^{\lambda\alpha\beta} = (\not{k}+m_c)\gamma^\lambda(\not{k}+m_c)\gamma^\alpha(\not{k}+m_c)\gamma^\beta(\not{k}+m_c) \quad (13)$$

$$\begin{aligned}
f^{\alpha\beta\mu\nu} &= (\not{k}+m_c)\gamma^\alpha(\not{k}+m_c)\gamma^\beta(\not{k}+m_c) \\
&\gamma^\mu(\not{k}+m_c)\gamma^\nu(\not{k}+m_c) \quad (14)
\end{aligned}$$

The correlation functions about DDJ/ψ and $DD^*\eta_c$ in Eqs. (7) and (10) have the same tensor structures, which can be expanded into the following structures,

$$\Pi_\mu(p, p') = \Pi_1(p^2, p'^2, q^2)p_\mu + \Pi_2(p^2, p'^2, q^2)p'_\mu \quad (15)$$

We choose the scalar amplitude $\Pi_1^{J/\psi(D)}$ and $\Pi_1^{D^*}$ to obtain $g_{DDJ/\psi}^{J/\psi(D)}$ and $g_{DD^*\eta_c}^{D^*}$, and use $\Pi_2^{J/\psi(D)}$ to obtain $g_{DD^*\eta_c}^{J/\psi(D)}$.

For the vertices DD^*J/ψ and $D^*D^*\eta_c$, their correlation functions in Eqs. (8) and (11) also have the same structures and can be written as follows,

$$\Pi_{\mu\nu}(p, p') = \Pi(p^2, p'^2, q^2)\epsilon_{\mu\nu\alpha\beta}p^\alpha p'^\beta \quad (16)$$

where $\epsilon_{\mu\nu\alpha\beta}$ is the 4-dimension Levi-Civita tensor. The invariant amplitude $\Pi^{J/\psi(D,D^*)}$ and $\Pi^{\eta_c(D^*)}$ are used to obtain $g_{DD^*J/\psi}^{J/\psi(D,D^*)}$ and $g_{D^*D^*\eta_c}^{\eta_c(D^*)}$, respectively.

There are three Lorentz indices in the correlation function about vertex D^*D^*J/ψ in Eq. (9), which leads to complicated tensor structures. For simplicity, we will contract the correlation functions with the metric tensor $g^{\mu\nu}$ to get the following

reduced correlation function with only one Lorentz index,

$$\begin{aligned}
g^{\mu\nu}\Pi_{\mu\nu\sigma}(p, p') &= \Pi_\sigma(p, p') \\
&= \Pi_1(p^2, p'^2, q^2)p_\sigma + \Pi_2(p^2, p'^2, q^2)p'_\sigma \quad (17)
\end{aligned}$$

Here Π_σ is the reduced correlation function which has above two structures. $\Pi_1^{J/\psi(D^*)}$ is used to obtain $g_{D^*D^*J/\psi}^{J/\psi(D^*)}$ in this work.

Finally, we use Π^{OPE} to represent all the scalar invariant amplitudes in the QCD side, and it can be divided into two parts,

$$\Pi^{\text{OPE}} = \Pi^{\text{pert}} + \Pi^{\text{non-pert}} \quad (18)$$

where Π^{pert} is the perturbative invariant amplitude and $\Pi^{\text{non-pert}}$ is the non-perturbative contributions including $\langle\bar{q}q\rangle$, $\langle g_s^2 G^2 \rangle$, $\langle\bar{q}g_s\sigma Gq\rangle$, $\langle f^3 G^3 \rangle$ and $\langle\bar{q}q\rangle\langle g_s^2 G^2 \rangle$. The perturbative part, $\langle g_s^2 G^2 \rangle$ and $\langle f^3 G^3 \rangle$ terms can be written in the following form by using the dispersion relation,

$$\Pi(p, p') = - \int_0^\infty \int_0^\infty \frac{\rho(s, u, q^2)}{(s-p^2)(u-p'^2)} ds du$$

where

$$\begin{aligned}
\rho(s, u, Q^2) &= \rho^{\text{pert}}(s, u, Q^2) + \rho^{\langle g_s^2 G^2 \rangle}(s, u, Q^2) \\
&+ \rho^{\langle f^3 G^3 \rangle}(s, u, Q^2) \quad (19)
\end{aligned}$$

Here $s = p^2$, $u = p'^2$ and $q = p - p'$. The QCD spectral density $\rho(s, u, q^2)$ will be obtained by using the Cutkosky's rules[41, 61](see Fig. 3). Besides of these above contributions, we also take into account the contributions from $\langle\bar{q}q\rangle$, $\langle\bar{q}g_s\sigma Gq\rangle$, and $\langle\bar{q}q\rangle\langle g_s^2 G^2 \rangle$. The Feynman diagrams for all of the condensate terms can be classified into two groups which can be seen in Figs. 4 and 5. As for the spectral density and contributions of $\langle\bar{q}q\rangle$, $\langle\bar{q}g_s\sigma Gq\rangle$, and $\langle\bar{q}q\rangle\langle g_s^2 G^2 \rangle$, only expressions for the vertex DDJ/ψ are shown in Appendixes A and B for simplicity.

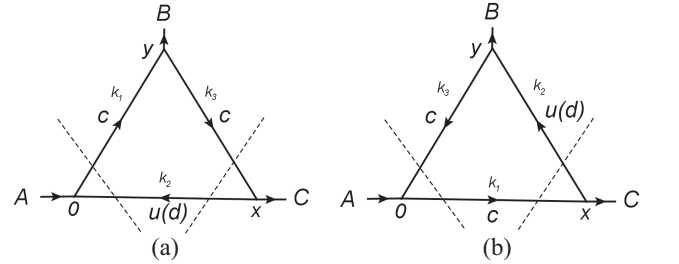
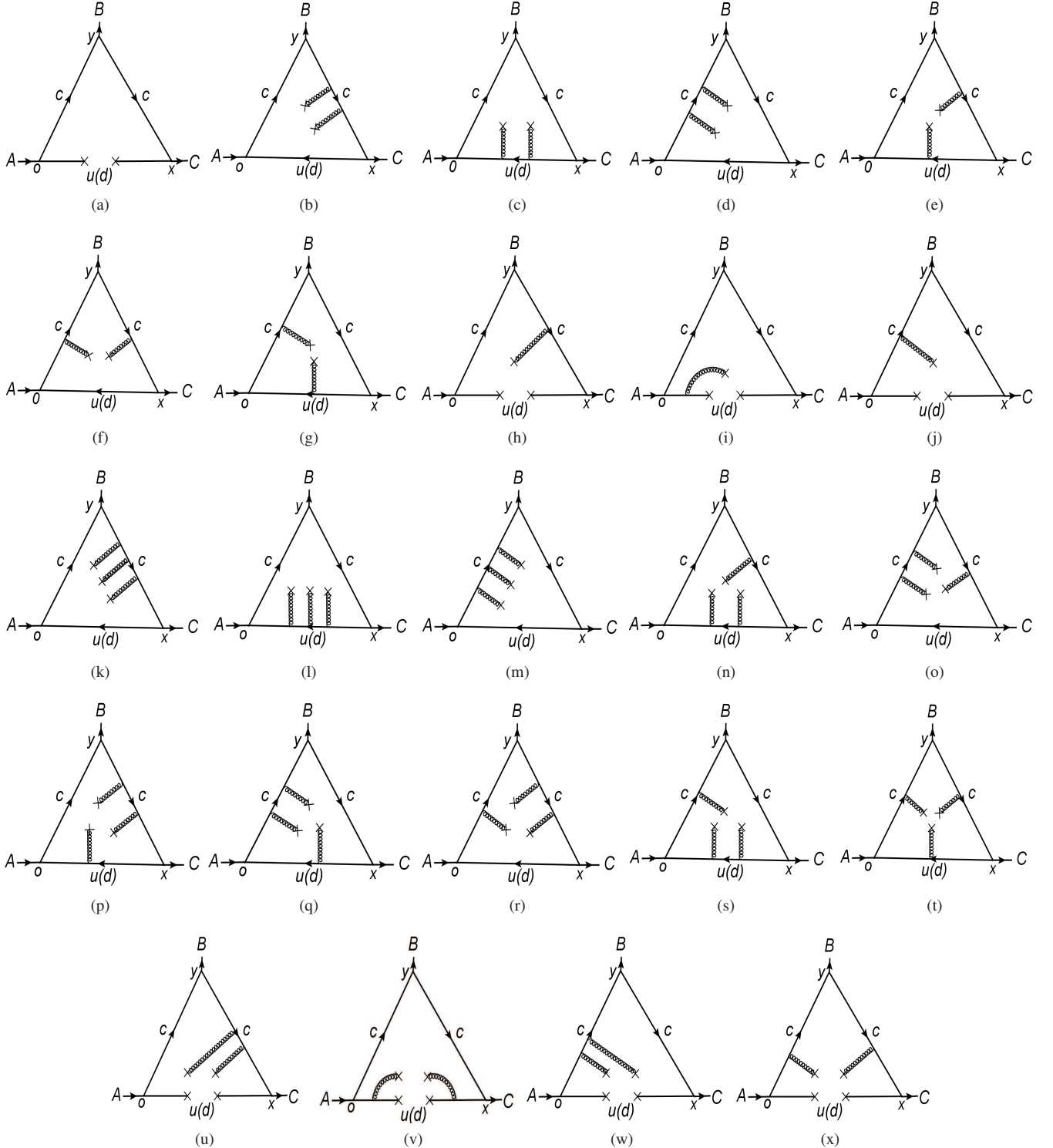


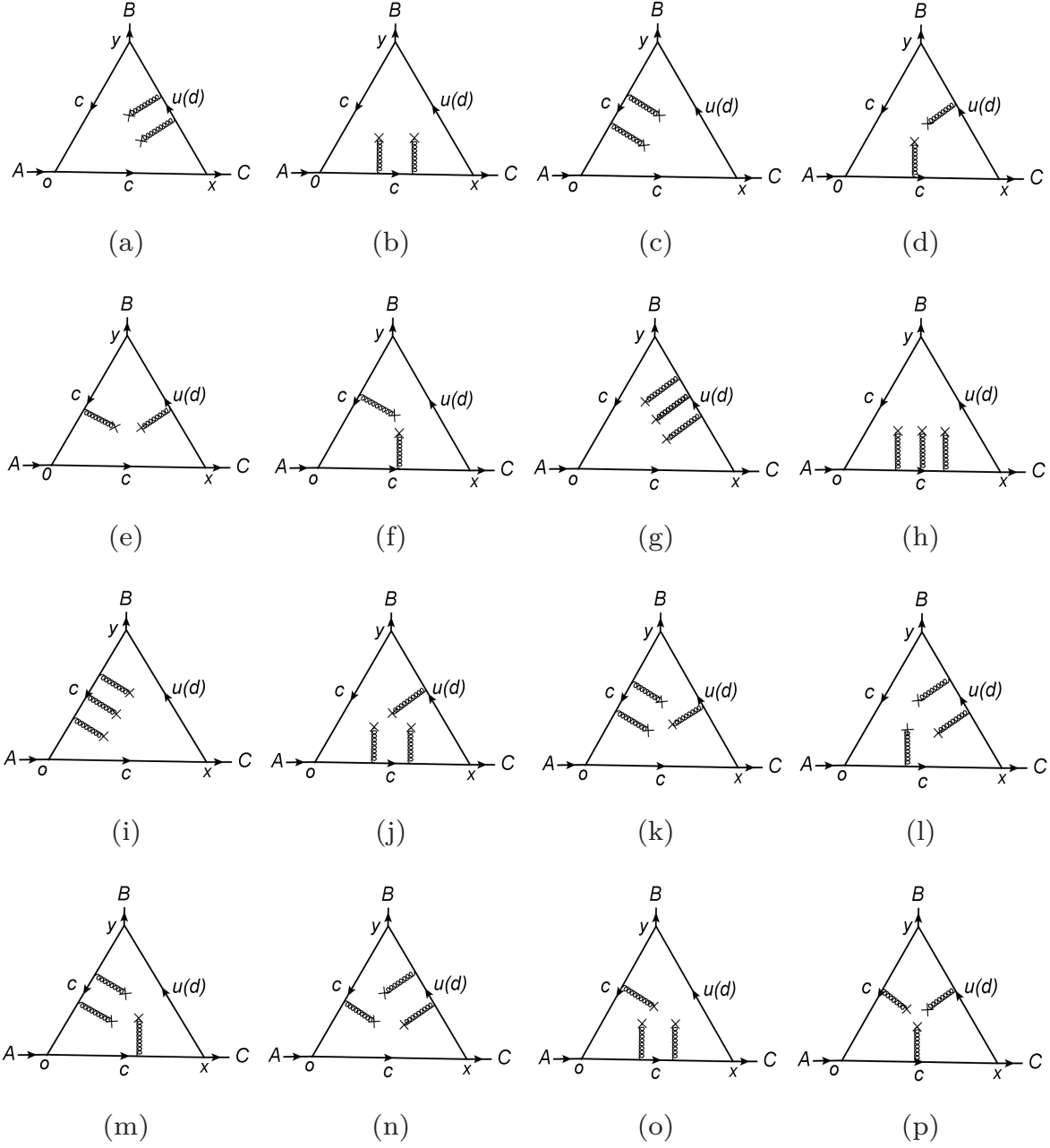
FIG. 3: The perturbative contributions for $J/\psi(\eta_c)$ (a) and $D(D^*)$ (b) off-shell. The dashed lines denote the Cutkosky cuts.

We take the change of variables $p^2 \rightarrow -P^2$, $p'^2 \rightarrow -P'^2$ and $q^2 \rightarrow -Q^2$ and perform the double Borel transform[62, 63] to the both phenomenological and QCD sides. The variables P^2 and P'^2 will be replaced by T_1^2 and T_2^2 , where T_1 and T_2 are the Borel parameters. In this article we take $T^2 = T_1^2$ and $T_2^2 = kT_1^2 = kT^2$, where k is a constant related to meson

FIG. 4: Contributions of the non-perturbative parts for $J/\psi(\eta_c)$ off-shell.

mass. It takes different values for different vertices and off-shell cases, and these values are represented in Table II. Then we match the phenomenological and the QCD sides using the quark-hardon duality. Finally, the sum rules for the strong form factor are obtained.

In order to eliminate the contributions of higher resonances and continuum states in Eq. (3), the threshold parameters s_0 and u_0 in dispersion integral will be introduced(see Eq. (20)). They fulfill the relations, $m_i^2 < s_0 < m_i'^2$ and $m_o^2 < u_0 < m_o'^2$, where subscript i and o represent incoming and outgoing

FIG. 5: Contributions of the non-perturbative parts for $D(D^*)$ off-shell.

mesons respectively. m and m' are the masses of the ground and first excited state of the mesons. There are relations $m' = m + \Delta$ for them, where Δ is usually taken as a value of $0.4 - 0.6$ GeV[56].

After these performing processes, the strong form factor

can be written as,

$$g(Q^2) = \frac{-\int \int \rho(s, u, Q^2) e^{-s/T^2} e^{-u/kT^2} ds du + \mathcal{B}\mathcal{B}[\Pi^{\text{non-pert}}]}{\frac{E}{(m_b^2 + Q^2)} e^{-m_A^2/T^2} e^{-m_C^2/kT^2}} \quad (20)$$

where the factors k and E have different expressions and are shown in Table. II. Besides, $\mathcal{B}\mathcal{B}[\]$ stands for the double

Borel transform. However, in order to obtain the strong coupling constants, it is necessary to extrapolate the results into time-like regions ($Q^2 < 0$). This process is realized by fitting the form factors with appropriate analytical functions and by setting the intermediate meson on-shell ($Q^2 = -m_{\text{on-shell}}^2$).

III. NUMERICAL RESULTS AND DISCUSSIONS

The hadronic parameters and meson decay constants in our calculation are taken as $m_D = 1.86 \text{ GeV}$ [64], $m_{D^*} = 2.01 \text{ GeV}$ [64], $m_{J/\psi} = 3.09 \text{ GeV}$ [64], $m_{\eta_c} = 2.98 \text{ GeV}$ [64], $m_{u(d)} = 0.006 \pm 0.001 \text{ GeV}$ [64], $m_c = 1.275 \pm 0.025 \text{ GeV}$ [64], $f_D = 0.210 \pm 0.011 \text{ GeV}$ [65], $f_{D^*} = 0.263 \pm 0.021 \text{ GeV}$ [65], $f_{J/\psi} = 0.418 \text{ GeV}$ [66], $f_{\eta_c} = 0.387 \text{ GeV}$ [66]. The vacuum condensates are taken as $\langle \bar{q}q \rangle = -(0.23 \pm 0.01)^3 \text{ GeV}^3$ [64], $\langle \bar{q}g_s \sigma G q \rangle = m_0^2 \langle \bar{q}q \rangle$ [64], $m_0^2 = 0.8 \pm 0.1 \text{ GeV}^2$ [67–69], $\langle g_s^2 G^2 \rangle = 0.88 \pm 0.15 \text{ GeV}^4$ [67–69], $\langle f^3 G^3 \rangle = (8.8 \pm 5.5) \text{ GeV}^2 \langle g_s^2 G^2 \rangle$ [67–69]. The continuum parameters in Eq. (20) are defined as $s_0 = (m_i + \Delta_i)^2$ and $u_0 = (m_o + \Delta_o)^2$. In this article, we uniformly take $\Delta_i = \Delta_o = 0.4, 0.5$ and 0.6 GeV for lower, intermediate, and upper values of the strong form factors, respectively.

The pole and continuum contributions play important roles for reliability of the final results. We can write,

$$\begin{aligned} \Pi_{\text{pole}}^{\text{OPE}}(T^2) &= - \int_{s_1}^{s_0} \int_{u_1}^{u_0} \rho^{\text{OPE}}(s, u, Q^2) e^{-\frac{s}{T^2}} e^{-\frac{u}{kT^2}} ds du \\ \Pi_{\text{cont}}^{\text{OPE}}(T^2) &= - \int_{s_0}^{\infty} \int_{u_0}^{\infty} \rho^{\text{OPE}}(s, u, Q^2) e^{-\frac{s}{T^2}} e^{-\frac{u}{kT^2}} ds du \end{aligned} \quad (21)$$

Then the pole and continuum contribution are defined as[56],

$$\begin{aligned} \text{Pole} &= \frac{\Pi_{\text{pole}}^{\text{OPE}}(T^2)}{\Pi_{\text{pole}}^{\text{OPE}}(T^2) + \Pi_{\text{cont}}^{\text{OPE}}(T^2)} \\ \text{Continuum} &= \frac{\Pi_{\text{cont}}^{\text{OPE}}(T^2)}{\Pi_{\text{pole}}^{\text{OPE}}(T^2) + \Pi_{\text{cont}}^{\text{OPE}}(T^2)} \end{aligned} \quad (22)$$

The contributions of pole and continuum for vertices DDJ/ψ , DD^*J/ψ , D^*D^*J/ψ , $DD^*\eta_c$ and $D^*D^*\eta_c$ are shown in Fig. 11. It is noted that QCD sum rule requires the pole contribution to be larger than 40%.

A. The form factors

The form factors will be obtained by Eq. (20), where the parameters k and E for all vertices and off-shell cases are shown in Table II. In this table, the function $\Lambda(m_{J/\psi}^2, m_{D^*}^2, Q^2)$ has the

TABLE II: The parameters k and E for different vertices and off-shell cases.

Vertices	off-shell	k	E
DDJ/ψ	J/ψ	1	$\frac{f_D^2 m_D^4 f_{J/\psi} m_{J/\psi}}{m_c^2}$
	D	$\frac{m_{J/\psi}^2}{m_{D^*}^2}$	$\frac{2f_D^2 m_D^4 f_{J/\psi} m_{J/\psi}}{m_c^2}$
DD^*J/ψ	J/ψ	$\frac{m_{D^*}^2}{m_D^2}$	$-\frac{f_D m_D^2 f_{D^*} m_{D^*} f_{J/\psi} m_{J/\psi}}{m_c}$
	D	$\frac{m_{J/\psi}^2}{m_{D^*}^2}$	
	D^*	$\frac{m_{J/\psi}^2}{m_D^2}$	
D^*D^*J/ψ	J/ψ	1	$f_{D^*}^2 m_{D^*}^2 f_{J/\psi} m_{J/\psi} (5 - \frac{Q^2}{2m_{D^*}^2})$
	D^*	$\frac{m_{J/\psi}^2}{m_D^2}$	$f_{D^*}^2 m_{D^*}^2 f_{J/\psi} m_{J/\psi} \Lambda(m_{J/\psi}^2, m_{D^*}^2, Q^2)$
$DD^*\eta_c$	η_c	$\frac{m_{D^*}^2}{m_D^2}$	$-\frac{f_D m_D^2 f_{D^*} m_{D^*} f_{\eta_c} m_{\eta_c}^2}{m_c^2}$
	D	$\frac{m_{\eta_c}^2}{m_{D^*}^2}$	
	D^*	$\frac{m_{\eta_c}^2}{m_D^2}$	$\frac{f_D m_D^2 f_{D^*} m_{D^*} f_{\eta_c} m_{\eta_c}^2 (m_{\eta_c}^2 + m_{D^*}^2 - m_D^2)}{2m_c^2 m_{D^*}^2}$
$D^*D^*\eta_c$	η_c	1	$-\frac{f_{D^*}^2 m_{D^*}^2 f_{\eta_c} m_{\eta_c}^2}{2m_c^2}$
	D^*	$\frac{m_{\eta_c}^2}{m_{D^*}^2}$	

following form,

$$\begin{aligned} \Lambda(m_{J/\psi}^2, m_{D^*}^2, Q^2) &= \frac{m_{D^*}^6 + m_{D^*}^4 (m_{J/\psi}^2 + Q^2)}{2m_{D^*}^2 m_{J/\psi}^2 Q^2} - \frac{Q^4}{2m_{D^*}^2 m_{J/\psi}^2} \\ &\quad - \frac{m_{D^*}^2 (m_{J/\psi}^4 - 10m_{J/\psi}^2 Q^2 + Q^4)}{2m_{D^*}^2 m_{J/\psi}^2 Q^2} \\ &\quad - \frac{m_{J/\psi}^6 - 9m_{J/\psi}^4 Q^2 - 9m_{J/\psi}^2 Q^4}{2m_{D^*}^2 m_{J/\psi}^2 Q^2} \end{aligned} \quad (23)$$

Fixing $Q^2 = 3 \text{ GeV}^2$ in Eq. (20), we find good stability of the results for these form factors. This stable region is called the Borel platform. In the Borel platform, the contributions of the total, perturbative and all vacuum condensate terms are shown in Fig. 12. Then we choose suitable T_0^2 in the Borel platform to meet the conditions of pole dominance($> 40\%$) and get the form factors in $Q^2 = 3 \text{ GeV}^2$. Finally, by taking different values of Q^2 , we can obtain the form factors $g(Q^2)$. The Borel platform, T_0^2 , pole contributions at T_0^2 and the range of Q^2 which are used to get form factors, are shown in Table III.

B. The coupling constants

The numerical results of form factors can be fitted uniformly by following analytical functions,

$$g(Q^2) = A_1 e^{-B_1 Q^2} + C_1 + C_2 Q^4 \quad (24)$$

TABLE III: The Borel platform, T_0^2 , the pole contributions and the range of Q^2 for all vertices.

Vertices	off-shell	Borel platform	$T_0^2(\text{GeV}^2)$	Pole(T_0^2)	$Q^2(\text{GeV}^2)$
DDJ/ψ	J/ψ	4.5 – 6.5	5.5	40.51%	1 – 8
	D	4 – 6	4.8	40.2%	4 – 10
DD^*J/ψ	J/ψ	5 – 7	6	40.21%	3.5 – 9.5
	D	5.5 – 7.5	6.5	42.5%	3 – 9
	D^*	4.5 – 6.5	5.5	42.16%	3 – 9
D^*D^*J/ψ	J/ψ	4.5 – 6.5	5.8	40.2%	1 – 7
	D^*	4 – 6	5	42.63%	5 – 11
$DD^*\eta_c$	η_c	4 – 6	4.8	40.51%	2 – 8
	D	3.5 – 5.5	4.5	40.03%	3 – 9
	D^*	2 – 4	2.5	40.11%	3 – 9
$D^*D^*\eta_c$	η_c	6 – 8	7	41.05%	3 – 9
	D^*	5 – 7	6	43.23%	3 – 9

where the parameters A_1 , B_1 , C_1 and C_2 are shown in Table IV. The fitting diagrams of strong form factors for each vertex and off-shell case are shown in Figs. 6–10. Then the strong form factors $g(Q^2)$ are extrapolated into the time-like region ($Q^2 < 0$) by Eq. 24, and on-shell condition is satisfied by setting $Q^2 = -m_{\text{on-shell}}^2$. For each vertex, we finally obtain the strong coupling constants of different off-shell cases which are shown in the last column of Table IV.

TABLE IV: The parameters for the analysis function and the strong coupling constants for different vertices and off-shell cases.

Vertex	off-shell	A_1	B_1	C_1	C_2	$g(Q^2 = -m_{\text{on-shell}}^2)$
DDJ/ψ	J/ψ	2.68	0.06	0	0.010	$5.83^{+0.70}_{-0.25}$
	D	2.37	0.16	0	0	$4.17^{+0.46}_{-0.06}$
DD^*J/ψ	J/ψ	2.13	0.04	0	0.004	$3.53^{+0.18}_{-0.56} \text{ GeV}^{-1}$
	D	2.36	0.11	0	0	$3.51^{+0.14}_{-0.05} \text{ GeV}^{-1}$
	D^*	1.95	0.15	0	0	$3.60^{+0.28}_{-0.01} \text{ GeV}^{-1}$
D^*D^*J/ψ	J/ψ	2.57	0.05	0	0.01	$5.06^{+0.65}_{-0.71}$
	D^*	2.60	0.17	0	0	$5.13^{+0.53}_{-0.11}$
$DD^*\eta_c$	η_c	0.30	0.24	1.19	0	$3.79^{+0.85}_{-0.14}$
	D	1.61	0.16	0	0	$2.75^{+0.07}_{-0.11}$
	D^*	1.72	0.24	-0.02	0	$4.49^{+0.25}_{-0.08}$
$D^*D^*\eta_c$	η_c	3.26	0.042	0	0.007	$5.28^{+0.73}_{-0.75} \text{ GeV}^{-1}$
	D^*	2.51	0.14	0	0	$4.45^{+0.12}_{-0.05} \text{ GeV}^{-1}$

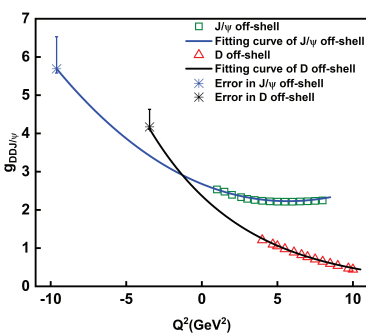


FIG. 6: The fitting curves of form factors for DDJ/ψ vertex in each off-shell case.

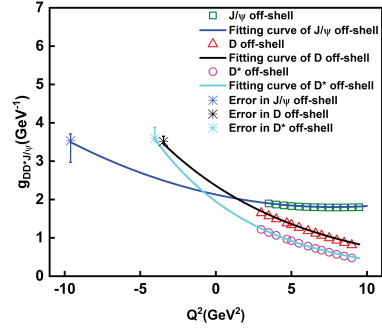


FIG. 7: The fitting curves of form factors for DD^*J/ψ vertex in each off-shell case.

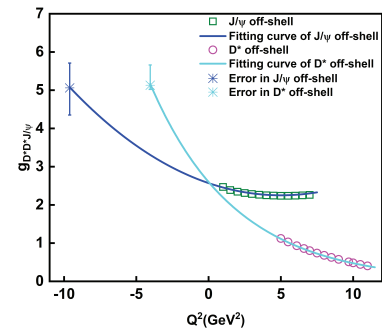


FIG. 8: The fitting curves of form factors for D^*D^*J/ψ vertex in each off-shell case.

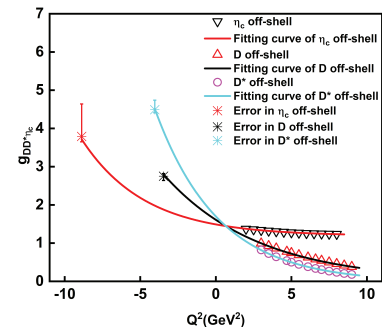


FIG. 9: The fitting curves of form factors for $DD^*\eta_c$ vertex in each off-shell case.

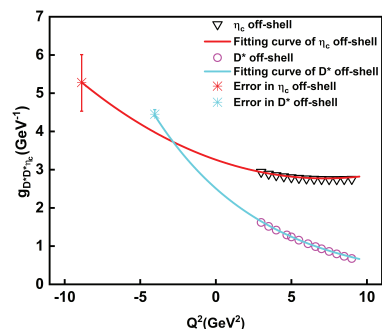


FIG. 10: The fitting curves of form factors for $D^*D^*\eta_c$ vertex in each off-shell case.

TABLE V: The strong coupling constants for all vertices.

Vertices	Present work	QCDSR	VMD	Other models
DDJ/ψ	$5.01^{+0.58}_{-0.16}$	5.8 ± 0.9 [56]	7.64 [31]	8.0 ± 0.5 [52]
DD^*J/ψ	$3.55^{+0.20}_{-0.21} \text{ GeV}^{-1}$	$4.0 \pm 0.6 \text{ GeV}^{-1}$ [56]	$8.0 \pm 0.6 \text{ GeV}^{-1}$ [32]	$4.05 \pm 0.25 \text{ GeV}^{-1}$ [52]
D^*D^*J/ψ	$5.10^{+0.59}_{-0.43}$	6.2 ± 0.9 [56]	7.64 [31]	8.0 ± 0.5 [52]
$DD^*\eta_c$	$3.68^{+0.39}_{-0.11}$	$5.23^{+1.80}_{-1.38}$ [57]	7.68 [71]	15.51 ± 0.45 [72]
$D^*D^*\eta_c$	$4.87^{+0.42}_{-0.40} \text{ GeV}^{-1}$	-	-	$9.76 \pm 0.32 \text{ GeV}^{-1}$ [72]

For each vertex, the strong coupling constants which are obtained by considering different off-shell cases, should be equal to each other. For $g_{DD^*J/\psi}$ as an example, it is shown by Table IV that the results of $g_{DD^*J/\psi}^D$, $g_{DD^*J/\psi}^{D^*}$ and $g_{DD^*J/\psi}^{J/\psi}$ for different off-shell cases are consistent with each other. Thus, by taking average value of the results for different off-shell cases, we can obtain the strong coupling constants for each

vertex. All of the final results are collected in Table V, where we can see that there is a significant difference between the results of QCDSR and those of other methods. Although the same method is employed in Refs.[56, 57], their results are not consistent well with ours. This difference may be due to the negligence of the contributions of high-dimension condensate terms in their studies.

According to SU(4) symmetry, the strong coupling constants of vertex DDJ/ψ and D^*D^*J/ψ satisfy the relation, $\frac{g_{DDJ/\psi}}{g_{DD^*J/\psi}} = 1$ [56]. And there are following relations, $\frac{g_{DDJ/\psi}}{g_{DD^*J/\psi}} = m_D$ [56], $\frac{g_{DD^*\eta_c}}{g_{D^*D^*\eta_c}} = \frac{m_D}{2}$, $g_{DD^*\eta_c} = g_2 \sqrt{m_{\eta_c}} m_D$, and $g_2 = 2.36 \text{ GeV}^{-3/2}$ in the heavy quark efficiency theory[70]. However, in charmed sector, the SU(4) and heavy-quark spin symmetry is only approximate, these relations are violated[56]. In our calculations, this violation is proved by the following relations about strong coupling constants, which are $\frac{g_{DDJ/\psi}}{g_{D^*D^*J/\psi}} \approx 0.98 < 1$, $\frac{g_{DDJ/\psi}}{g_{DD^*J/\psi}} \approx 1.41 < m_D$, $\frac{g_{DD^*\eta_c}}{g_{D^*D^*\eta_c}} \approx 0.76 < \frac{m_D}{2}$ and $g_{DD^*\eta_c} = 3.68 < g_2 \sqrt{m_{\eta_c}} m_D$.

rules, where all off-shell cases are considered for each vertex. Under this physical sketch, the strong form factors are firstly calculated in the space-like ($Q^2 > 0$) regions, and then are fitted into appropriate functions. By extrapolating these functions into the time-like ($Q^2 < 0$) regions and taking $Q^2 = -m_{\text{on-shell}}^2$, we obtain the strong coupling constants. For each vertex, we take the average value of the strong coupling constants for all off-shell cases as the final results. These strong form factors and coupling constants are important in describing the dynamic behavior of hadrons, which can be used to analyze the production processes of the exotic particles.

IV. CONCLUSIONS

In this work, we analyze the strong vertices DDJ/ψ , DD^*J/ψ , D^*D^*J/ψ , $DD^*\eta_c$, $D^*D^*\eta_c$ by different QCD sum

Appendix A: Full expressions of the perturbative, $\langle g_s^2 G^2 \rangle$ and $\langle f^3 G^3 \rangle$ spectral density for J/ψ and D off-shell cases.

$$\rho^{pert(J/\psi)} = -\frac{3}{4\pi^2[(Q^2 + s + u)^2 - 4su]^{5/2}} \{-m_c^6 Q^2(Q^2 + s - u) + m_c^4 Q^2[-2Q^4 - Q^2(4s + u) \\ - 2s^2 + su + u^2] + m_c^2 [Q^6(s + u) + Q^4(3s^2 + 2u^2) + Q^2(3s^3 - 4s^2u + u^3) \\ + s(s - u)^3] + su[Q^4s + Q^2(2s^2 - su - u^2) + (s - u)^3]\} \quad (25)$$

$$\rho^{\langle g_s^2 G^2 \rangle (J/\psi)} = \frac{\langle g_s^2 G^2 \rangle}{96\pi^2[(Q^2 + s + u)^2 - 4su]^{7/2}} \{ 12m_c^4[2Q^4s - Q^2(s^2 - 4su + 5u^2) - 3s^3 + s^2u - 3su^2 + 5u^3] + 6m_c^2[2Q^8 + 2Q^6(4s + u) + Q^4(7s^2 + 2su - 7u^2) - 2Q^2(s^3 + s^2u - su^2 + u^3) - 3s^4 - 2s^3u - 2s^2u^2 + 2su^3 + 5u^4] + 5Q^{10} + Q^8(13s + 15u) + 2Q^6(s^2 + 3su + 14u^2) - 2Q^4(11s^3 + 6s^2u - 5su^2 - 22u^3) + Q^2(-23s^4 + 18s^3u - 18su^3 + 39u^4) - (s - u)^2(7s^3 - 7s^2u + 9su^2 - 13u^3) \} \quad (26)$$

$$\rho^{\langle f^3 G^2 \rangle (J/\psi)} = -\frac{\langle f^3 G^2 \rangle}{192\pi^2[(Q^2 + s + u)^2 - 4su]^{9/2}} \{ 126m_c^5 Q^6(Q^2 + s - u) - 9m_c^4[35Q^8 + Q^6(36s - 35u) - 3Q^4(s^2 - su + 6u^2) - Q^2(2s^3 + 3s^2u + 33su^2 - 48u^3) + (s - u)^2(2s^2 + su - 18u^2)] + 18m_c^3 Q^4[Q^6 - 2Q^4(2s + 3u) - Q^2(11s^2 - 12su + u^2) - 6(s - u)^3] + m_c^2[-142Q^{10} - 16Q^8(4s - 7u) + 3Q^6(126s^2 - 134su + 89u^2) + Q^4(386s^3 - 558s^2u + 1359su^2 - 527u^3) + Q^2(92s^4 + 100s^3u + 873s^2u^2 - 874su^3 - 571u^4) + (s - u)^2(6s^3 + 12s^2u + 233su^2 - 31u^3)] - 9m_c Q^2[Q^8(s + u) + Q^6(s^2 - 6su - u^2) - 3Q^4(s^3 + s^2u - 3su^2 + u^3) - Q^2(s - u)^3(5s + u) - 2(s - u)^5] + Q^{10}(77s + 52u) + Q^8(229s^2 - 35su + 124u^2) + Q^6(218s^3 - 115s^2u + 405su^2 + 25u^3) + Q^4(50s^4 + 125s^3u + 357s^2u^2 + 58su^3 - 122u^4) - Q^2(23s^5 - 159s^4u + 97s^3u^2 - 311s^2u^3 + 317su^4 + 83u^5) - (s - u)^2(7s^4 + 8s^3u - 24s^2u^2 - 144su^3 + 8u^4) \} \quad (27)$$

$$\rho^{pert(D)} = -\frac{3}{4\pi^2[(Q^2 + s + u)^2 - 4su]^{5/2}} \{ -2m_c^6u^2 + m_c^4u[Q^4 + Q^2(2s + 5u) + s^2 - 5su + 4u^2] + m_c^2[Q^8 + 4Q^6(s + u) + Q^4(6s^2 + 4su + 5u^2) + 2Q^2(2s^3 - 2s^2u + u^3) + s(s - 2u)(s - u)^2] + Q^2su[Q^4 + Q^2(2s + u) + s(s - u)] \} \quad (28)$$

$$\rho^{\langle g_s^2 G^2 \rangle (D)} = \frac{\langle g_s^2 G^2 \rangle}{48\pi^2[(Q^2 + s + u)^2 - 4su]^{7/2}} \{ 12m_c^4[Q^6 + Q^4(s - 3u) + Q^2(-s^2 - 4su + u^2) - s(s^2 + 3su + u^2)] - 6m_c^2[Q^8 - 2Q^6u - 2Q^4s^2 + Q^2u^2(5u - 2s) + s^4 + 2s^3u - 5su^3 + 2u^4] + 2Q^{10} + 3Q^8(2s + u) + 2Q^6(2s^2 + u^2) + Q^4(-4s^3 - 2s^2u + 6su^2 + 8u^3) - 2Q^2(3s^4 - 4s^3u + 5s^2u^2 + 2su^3 - 6u^4) - (s - u)^3(2s^2 - su + 5u^2) \} \quad (29)$$

$$\rho^{\langle f^3 G^2 \rangle (D)} = \frac{\langle f^3 G^2 \rangle}{192\pi^2[(Q^2 + s + u)^2 - 4su]^{9/2}} \{ 9m_c^4[7Q^8 + Q^6(23s - 32u) + 3Q^4(9s^2 - 9su + 14u^2) + Q^2(13s^3 + 27s^2u + 57su^2 - 2u^3) + 2s^4 + 22s^3u + 42s^2u^2 + 17su^3 - 83u^4] + 2m_c^2[15Q^{10} + Q^8(91s + 109u) + Q^6(174s^2 - 325su - 209u^2) + Q^4(126s^3 - 717s^2u + 132su^2 - 545u^3) + Q^2(19s^4 - 178s^3u - 90s^2u^2 - 915su^3 - 102u^4) - (s - u)^2(9s^3 - 87s^2u - 253su^2 - 140u^3)] - 3Q^{12} - Q^{10}(51s + 32u) + Q^8(-115s^2 + 189su - 7u^2) + Q^6(-75s^3 + 115s^2u - 290su^2 + 242u^3) + 2Q^4u(-192s^3 + 18s^2u + 6su^2 + 179u^3) + 2Q^2(s^5 - 126s^4u - 27s^3u^2 - 225s^2u^3 + 325su^4 + 52u^5) - 2(s - u)^3(3s^3 - 4s^2u - 42su^2 - 17u^3) \} \quad (30)$$

Appendix B: Full expressions about the condensate terms $\langle \bar{q}q \rangle$, $\langle \bar{q}g_s \sigma G q \rangle$ and $\langle \bar{q}q \rangle \langle g_s^2 G^2 \rangle$ for J/ψ off-shell.

$$\Pi^{\langle\bar{q}q\rangle(J/\psi)} = \langle\bar{q}q\rangle \frac{m_c}{(p^2 - m_c^2)(p'^2 - m_c^2)} \quad (31)$$

$$\begin{aligned} \Pi^{\langle\bar{q}g_s\sigma Gq\rangle(J/\psi)} &= -\langle\bar{q}g_s\sigma Gq\rangle \left[\frac{m_c}{4(p^2 - m_c^2)^2(p'^2 - m_c^2)} \right. \\ &\quad \left. + \frac{2m_c^4}{(p^2 - m_c^2)(p'^2 - m_c^2)^3} + \frac{m_c}{2(p^2 - m_c^2)(p'^2 - m_c^2)^2} \right] \end{aligned} \quad (32)$$

$$\begin{aligned} \Pi^{\langle\bar{q}q\rangle\langle g_s^2 G^2\rangle(J/\psi)} &= \langle\bar{q}q\rangle \langle g_s^2 G^2 \rangle \left[\frac{m_c^3}{6(p^2 - m_c^2)(p'^2 - m_c^2)^4} \right. \\ &\quad \left. + \frac{m_c^5}{6(p^2 - m_c^2)(p'^2 - m_c^2)^5} + \frac{m_c^3}{12(p^2 - m_c^2)^4(p'^2 - m_c^2)} \right. \\ &\quad \left. + \frac{m_c}{12(p^2 - m_c^2)(p'^2 - m_c^2)^3} + \frac{m_c}{24(p^2 - m_c^2)^2(p'^2 - m_c^2)^2} \right] \end{aligned} \quad (33)$$

Appendix C: The pole and continuum contributions, and the contributions of different condensate terms for all vertices.

- [1] B. Aubert *et al.* [BaBar], Phys. Rev. Lett. **90**, 242001 (2003).
[2] B. Aubert *et al.* [BaBar], Phys. Rev. Lett. **95**, 142001 (2005).
[3] K. Abe *et al.* [Belle], Phys. Rev. Lett. **94**, 182002 (2005).
[4] B. Aubert *et al.* [BaBar], Phys. Rev. D **74**, 091103 (2006).
[5] T. Aaltonen *et al.* [CDF], Phys. Rev. Lett. **102**, 242002 (2009).
[6] C. P. Shen *et al.* [Belle], Phys. Rev. Lett. **104**, 112004 (2010).
[7] A. Bondar *et al.* [Belle], Phys. Rev. Lett. **108**, 122001 (2012).
[8] T. Xiao, S. Dobbs, A. Tomaradze and K. K. Seth, Phys. Lett. B **727**, 366-370 (2013).
[9] R. Aaij *et al.* [LHCb], Phys. Rev. Lett. **112**, no.22, 222002 (2014).
[10] K. Chilikin *et al.* [Belle], Phys. Rev. D **90**, no.11, 112009 (2014).
[11] R. Aaij *et al.* [LHCb], Phys. Rev. Lett. **115**, 072001 (2015).
[12] T. Aaltonen *et al.* [CDF], Mod. Phys. Lett. A **32**, no.26, 1750139 (2017).
[13] R. Aaij *et al.* [LHCb], Phys. Rev. Lett. **119**, no.11, 112001 (2017).
[14] T. Branz, T. Gutsche and V. E. Lyubovitskij, Phys. Rev. D **80**, 054019 (2009).
[15] N. Mahajan, Phys. Lett. B **679**, 228-230 (2009).
[16] X. Liu, Phys. Lett. B **680**, 137-140 (2009).
[17] X. Liu, Z. G. Luo, Y. R. Liu and S. L. Zhu, Eur. Phys. J. C **61**, 411-428 (2009).
[18] J. M. Dias, F. S. Navarra, M. Nielsen and C. Zanetti, arXiv:1311.7591.
[19] Z. G. Wang, Eur. Phys. J. C **74**, no.7, 2963 (2014).
[20] Z. G. Wang and T. Huang, Nucl. Phys. A **930**, 63-85 (2014).
[21] Z. J. Zhao and D. M. Pan, arXiv:1104.1838.
[22] S. J. Brodsky, D. S. Hwang and R. F. Lebed, Phys. Rev. Lett. **113**, no.11, 112001 (2014).
[23] D. Besson *et al.* [CLEO], Phys. Rev. D **68**, 032002 (2003) [erratum: Phys. Rev. D **75**, 119908 (2007)].
[24] P. Krokovny *et al.* [Belle], Phys. Rev. Lett. **91**, 262002 (2003).
[25] P. A. Zyla *et al.* [Particle Data Group], PTEP **2020**, no.8, 083C01 (2020).
[26] M. Z. Liu, X. Z. Ling, L. S. Geng, En-Wang and J. J. Xie, Phys. Rev. D **106**, no.11, 114011 (2022).
[27] J. J. de Swart, Rev. Mod. Phys. **35**, 916-939 (1963).
[terratum: Rev. Mod. Phys. **37**, 326-326 (1965)].
[28] B. Holzenkamp, K. Holinde and J. Speth, Nucl. Phys. A **500**, 485-528 (1989).
[29] F. Carvalho, F. O. Duraes, F. S. Navarra, M. Nielsen and F. M. Steffens, Eur. Phys. J. C **18**, 127-136 (2000).
[30] S. G. Matinyan and B. Muller, Phys. Rev. C **58**, 2994-2997 (1998).
[31] Z. w. Lin and C. M. Ko, Phys. Rev. C **62**, 034903 (2000).
[32] Y. s. Oh, T. Song and S. H. Lee, Phys. Rev. C **63**, 034901 (2001).
[33] R. L. Altmeyer, M. Gockeler, R. Horsley, E. Laermann, G. Schierholz and P. M. Zerwas, Nucl. Phys. B Proc. Suppl. **34**, 373-375 (1994).
[34] T. Doi, Y. Kondo and M. Oka, Phys. Rept. **398**, 253-279 (2004).
[35] V. V. Braguta and A. I. Onishchenko, Phys. Lett. B **591**, 267-276 (2004).
[36] V. V. Braguta and A. I. Onishchenko, Phys. Rev. D **70**, 033001 (2004).
[37] C. Aydin and A. H. Yilmaz, Mod. Phys. Lett. A **19**, 2129-2134 (2004).
[38] C. Aydin, M. Bayar and A. H. Yilmaz, Phys. Rev. D **73**, 074020 (2006).
[39] M. E. Bracco, M. Chiapparini, F. S. Navarra and M. Nielsen, Phys. Lett. B **659**, 559-564 (2008).
[40] M. E. Bracco and M. Nielsen, Phys. Rev. D **82**, 034012 (2010).
[41] Z. G. Wang, Phys. Rev. D **89**, no.3, 034017 (2014).
[42] G. L. Yu, Z. Y. Li and Z. G. Wang, Eur. Phys. J. C **75**, no.6, 243 (2015).
[43] K. Azizi and H. Sundu, J. Phys. G **38**, 045005 (2011).
[44] K. Azizi, Y. Sarac and H. Sundu, Phys. Rev. D **90**, no.11, 114011 (2014).
[45] A. Khodjamirian, T. Mannel, N. Offen and Y. M. Wang, Phys. Rev. D **83**, 094031 (2011).
[46] A. Khodjamirian, C. Klein, T. Mannel and Y. M. Wang, JHEP **09**, 106 (2011).
[47] A. Khodjamirian, B. Melić, Y. M. Wang and Y. B. Wei,

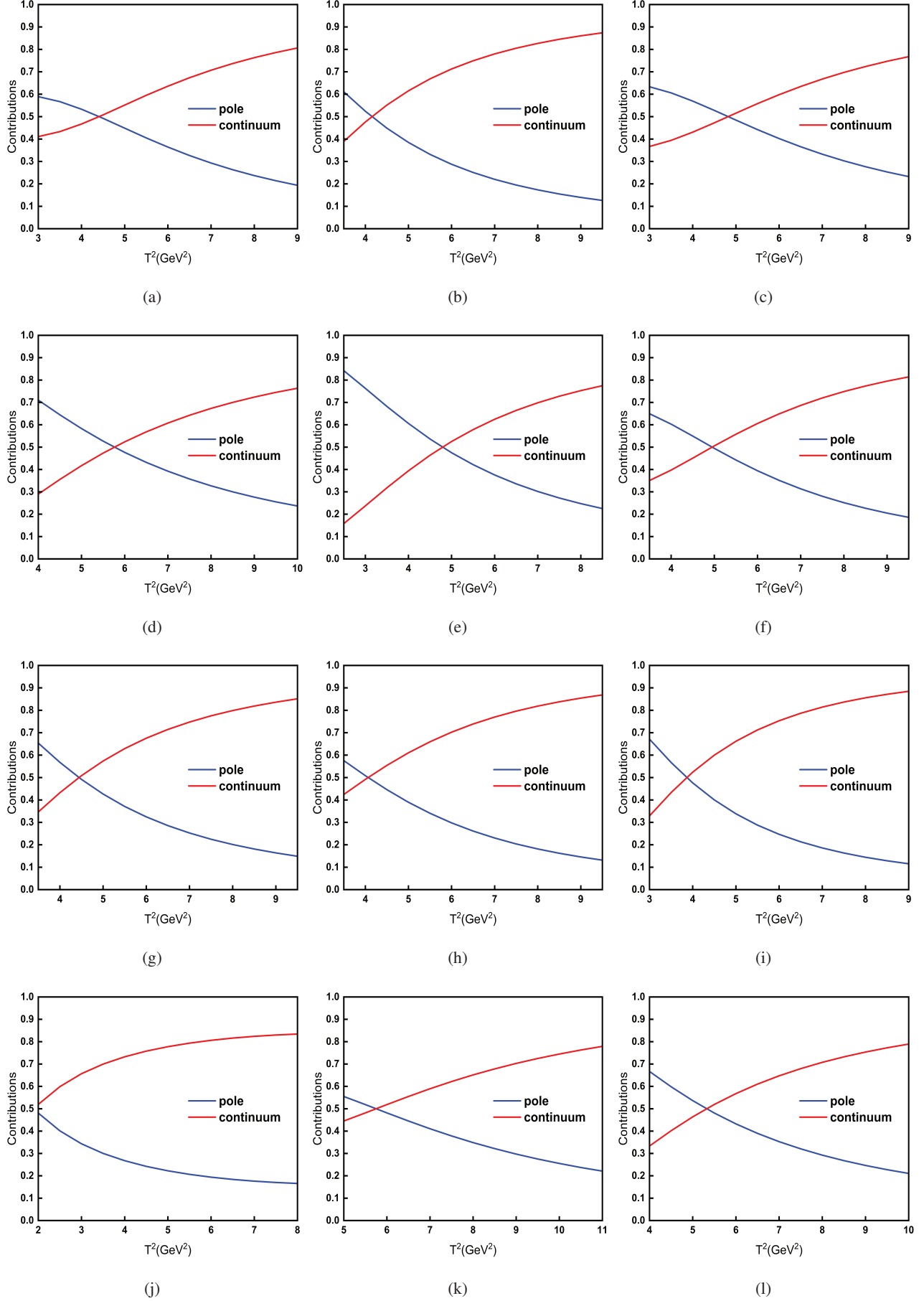


FIG. 11: The pole and continuum contributions with variation of the Borel parameter T^2 for DDJ/ψ (a-b), DD^*J/ψ (c-e), D^*D^*J/ψ (f-g), $DD^*\eta_c$ (h-j), $D^*D^*\eta_c$ (k-l).

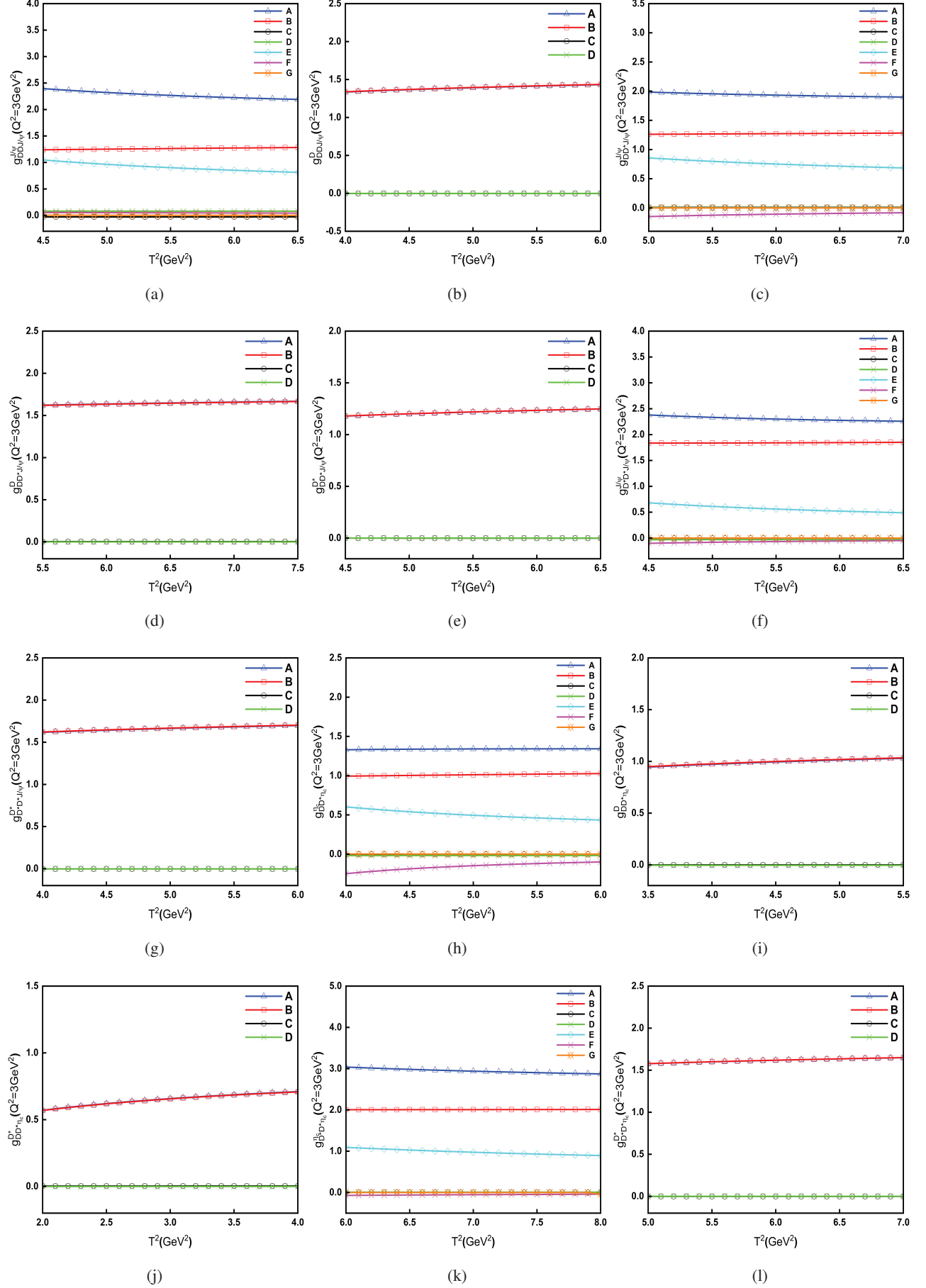


FIG. 12: The contributions of different vacuum condensate terms with variation of the Borel parameter T^2 for DDJ/ψ (a-b), DD^*J/ψ (c-e), D^*D^*J/ψ (f-g), $DD^*\eta_c$ (h-j), $D^*D^*\eta_c$ (k-l), where A-G denote the total, perturbative term, $\langle g_s^2 G^2 \rangle$, $\langle f^3 G^3 \rangle$, $\langle \bar{q}q \rangle$, $\langle \bar{q}g_s \sigma G q \rangle$, and $\langle \bar{q}q \rangle \langle g_s^2 G^2 \rangle$ contributions.

- JHEP **03**, 016 (2021).
- [48] T. M. Aliev and M. Savci, Phys. Rev. D **88**, no.5, 056021 (2013).
- [49] T. M. Aliev and M. Savci, Phys. Rev. D **90**, no.9, 096012 (2014).
- [50] Z. G. Wang and Z. B. Wang, Chin. Phys. Lett. **25**, 444-446 (2008).
- [51] Z. H. Li, T. Huang, J. Z. Sun and Z. H. Dai, Phys. Rev. D **65**, 076005 (2002).
- [52] A. Deandrea, G. Nardulli and A. D. Polosa, Phys. Rev. D **68**, 034002 (2003).
- [53] M. A. Shifman, A. I. Vainshtein and V. I. Zakharov, Nucl. Phys. B **147**, 448-518 (1979).
- [54] G. L. Yu, Z. G. Wang and Z. Y. Li, Eur. Phys. J. C **79**, no.9, 798 (2019).
- [55] Z. Y. Li, Z. G. Wang and G. L. Yu, Mod. Phys. Lett. A **31**, no.06, 1650036 (2016).
- [56] M. E. Bracco, M. Chiapparini, F. S. Navarra and M. Nielsen, Prog. Part. Nucl. Phys. **67**, 1019-1052 (2012).
- [57] B. O. Rodrigues, M. E. Bracco and C. M. Zanetti, Nucl. Phys. A **966**, 208-223 (2017).
- [58] C. J. Xiao, Y. Huang, Y. B. Dong, L. S. Geng and D. Y. Chen, Phys. Rev. D **100**, no.1, 014022 (2019).
- [59] Q. Wu and D. Y. Chen, Phys. Rev. D **104**, no.7, 074011 (2021).
- [60] Z. G. Wang and Z. Y. Di, Eur. Phys. J. A **50**, 143 (2014).
- [61] Z. G. Wang, Nucl. Phys. B **973**, 115579 (2021).
- [62] B. L. Ioffe and A. V. Smilga, Phys. Lett. B **114**, 353-358 (1982).
- [63] B. L. Ioffe and A. V. Smilga, Nucl. Phys. B **216**, 373-407 (1983).
- [64] M. Tanabashi *et al.* [Particle Data Group], Phys. Rev. D **98**, no.3, 030001 (2018).
- [65] Z. G. Wang, Eur. Phys. J. C **75**, 427 (2015).
- [66] D. Bećirević, G. Duplančić, B. Klajn, B. Melić and F. Sanfilippo, Nucl. Phys. B **883**, 306-327 (2014).
- [67] S. Narison, Phys. Lett. B **693**, 559-566 (2010) [erratum: Phys. Lett. B **705**, 544-544 (2011)].
- [68] S. Narison, Phys. Lett. B **706**, 412-422 (2012).
- [69] S. Narison, Phys. Lett. B **707**, 259-263 (2012).
- [70] Y. H. Lin, C. W. Shen, F. K. Guo and B. S. Zou, Phys. Rev. D **95**, no.11, 114017 (2017).
- [71] Q. Wang, X. H. Liu and Q. Zhao, Phys. Lett. B **711**, 364-370 (2012).
- [72] W. Lucha, D. Melikhov, H. Sazdjian and S. Simula, Phys. Rev. D **93**, no.1, 016004 (2016).